Nanofiber composite membranes with low equivalent weight perfluorosulfonic acid polymers†

Jonghyun Choi,[a] Kyung Min Lee,[a] Ryszard Wycisk,[a] Peter N. Pintauro*[b] and Patrick T. Mather[c]

Received 17th February 2010, Accepted 5th May 2010
DOI: 10.1039/c0jm00441c

Two low equivalent weight perfluorosulfonic acid (PFSA) polymers (825 EW and 733 EW) were successfully electrospun into nanofibers by adding as little as 0.3 wt% of high molecular weight poly(ethylene oxide) as a carrier polymer. The electrospun fiber morphology transitioned from cylindrical filaments to flat ribbons as the total concentration of PFSA + carrier in solution increased from 5 wt% to 30 wt%. PFSA nanofiber mats were transformed into defect-free dense membranes using a four-step procedure: (i) annealing the PFSA polymer during which time intersecting fibers were welded to one another at cross points (ii) mechanically compacting the mats to increase the volume fraction of nanofibers to ~75%, (iii) imbibing an inert polymer, Norland Optical Adhesive (NOA) 63, into the mats (to fill entirely the void space between nanofibers) and then crosslinking the NOA with UV light, and (iv) removing the poly(ethylene oxide) carrier polymer by boiling the membrane in 1.0 M H_2SO_4 and then in deionized water. The resulting membranes exhibited higher proton conductivities than that of commercial Nafion 212 membrane (0.16 S/cm at 80 °C and 80% relative humidity and 0.048 S/cm at 80 °C and 50% relative humidity for a membrane with 733 EW nanofibers), with low water swelling (liquid water swelling of 18% for membrane with high conductivity). The proton conductivity of both EW nanofiber composite membranes increased linearly with the PFSA nanofiber volume fraction, whereas gravimetric water swelling was less than expected, based on the volume fraction of ionomer. There was a significantly improvement in the mechanical properties of the nanofiber composite membranes, as compared to recast homogeneous PFSA films.

Introduction

There is a continuing need for high performance polymeric membranes for hydrogen/air and direct methanol proton-exchange membrane (PEM) fuel cells. Such new membranes must possess the requisite transport properties (*e.g.*, high proton conductivity and low gas permeability) and have outstanding durability (*i.e.*, mechanical, chemical, and thermal stability). Strategies for fabricating new membranes for electrochemical applications have focused to a large extent on: (1) the synthesis of new high ion-exchange capacity (IEC) polymers,[1,2] (2) the use of block copolymers which self assemble into nano-phases,[3,4] (3) the combination of two different polymers or one polymer and an inorganic additive (*e.g.*, silica) in a single membrane by blending/mixing followed by solution casting,[5,6] and (4) impregnating a functional polymer into a microporous inert support, where the support provides mechanical properties that the functional polymer does not possess.[7–9] There have been some successes with these approaches, but they all have limitations. For example, the use of block copolymers is limited by polymer chemistry and by the availability of a suitable solvent for solution casting membranes from the resulting block material (this is particularly troublesome when the blocks differ significantly from one another in terms of physical properties, *e.g.*, hydrophilic and hydrophobic blocks). Also, there is no guarantee as to the desired level of organization of phase-separated domains in a block copolymer after membrane casting. Similarly, it is difficult to create polymer blends with a good dispersion of one polymer in the second, *i.e.*, where the domain size of the minor blend component is 1 μm or less. With poorly dispersed blends, there is no control of membrane swelling and no improvement in mechanical properties.

Nanofiber composite proton conducting membranes utilize a "forced assembly" fabrication scheme to generate, a highly desirable, phase-separated polymer morphology. In these membranes, a three-dimensional network of interconnected electrospun ionomeric nanofibers is embedded in an inert (uncharged) polymer matrix.[10–12] High proton conductivity is insured by maintaining a sufficiently large number of highly charged (high ion-exchange capacity) nanofibers in the membrane. The inert/hydrophobic polymer that surrounds all ionomeric/hydrophilic nanofibers, restricts fiber swelling and provides overall mechanical strength to the final membrane. Membranes with this new morphology have been prepared[10] using sulfonated poly(arylene ether sulfone) with an ion-exchange capacity of between 2.1 and 2.5 mmol/g; in some cases, the sulfonated polymer fibers were loaded with sulfonated molecular silica (sulfonated polyhedral oligomeric

[a]*Department of Chemical Engineering, Case Western Reserve University, Cleveland, OH, 44106, USA*
[b]*Department of Chemical and Biomolecular Engineering, Vanderbilt University, Nashville, TN, 37235, USA. E-mail: peter.pintauro@vanderbilt.edu; Fax: +615.343.7951; Tel: +615.343.3878*
[c]*Syracuse Biomaterials Institute, Biomedical and Chemical Engineering, Department, Syracuse University, Syracuse, NY, 13244, USA*
† This paper is part of a *Journal of Materials Chemistry* themed issue on proton transport for fuel cells. Guest editors: Sossina Haile and Peter Pintauro.

silsesquioxane).[11,12] A four-step procedure for membrane fabrication was employed comprising: (1) nanofiber electrospinning of the ionomer into a mat of uniform thickness and nanofiber volume fraction, (2) mat compaction to increase the density of nanofibers, (3) welding of intersecting nanofibers at their crossing points to generate a 3-D interconnected fiber network, and (4) embedding into the mat and then UV-curing Norland Optical Adhesive (NOA) 63 as the inter/uncharged matrix polymer (NOA63 is a UV-curable polyurethane pre-polymer with water-like viscosity that is easily imbibed into the membrane and then cured by UV light exposure, as discussed elsewhere[10]).

In the present paper we have extended the nanofiber composite membrane fabrication scheme to low equivalent weight (EW) perfluorosulfonic acid (PFSA) polymers from 3M Corporation (825 EW and 733 EW polymers, with corresponding ion-exchange capacities of 1.21 and 1.36 mmol/g, respectively). The chemical structure of these polymers is shown in Fig. 1. The perfluoroether sulfonic acid side chains lack branching and are somewhat shorter as compared to that of DuPont's Nafion. Additional information on these polymers (including the general synthesis scheme, membrane physical property data, and fuel cell performance results) can be found in ref. 13 and 14. Methods for electrospinning the 3M Corporation polymers are presented below, along with the procedure for transforming an ionomeric nanofiber mat into a functioning ion-exchange membrane with properties suitable for use in a PEM fuel cell.

Experimental

Electrospinning solution preparation

PFSA electrospinning reports in the literature have focused on Nafion® polymer. Researchers were unsuccessful in electrospinning a solution of neat Nafion in any of the usual membrane casting solvents (*e.g.*, alcohol/water or dimethylacetamide) because of an insufficient number of polymer chain entanglements (a consequence of the fact that Nafion does not molecularly dissolve in typical solvents, but rather forms a micellar solution). Thus, Nafion was electrospun in the presence of a high molecular weight polymer carrier, such as poly(ethylene oxide) (PEO), poly(acrylic acid) (PAA), or poly(vinyl alcohol) (PVA). Laforgue *et al.*[15] electrospun Nafion with either 16+ wt% PEO or 15+ wt% PVA and Chen and co-workers[16] claimed that Nafion could not be electrospun without a minimum of 25 wt% PAA (all concentrations were relative to the amount of Nafion polymer in the spinning solution). Such high carrier concentrations in electrospun ionomer nanofibers are undesirable; the uncharged carrier polymer will dilute the ion-exchange material and the carrier polymer may be prone to degradation in certain membrane applications. Extraction of the carrier polymer after electrospinning may be easily accomplished (*e.g.*, for water soluble carriers), but the fibers could be significantly weakened if the carrier concentration is too high. The present authors have also performed electrospinning experiments with Nafion polymer[12] (1100 EW PFSA). From preliminary experiments it was found that a well-formed nanofiber mat, with no beads, could be formed using as little as 1 wt% poly(ethylene oxide). This result was used as the basis for preparing electrospinning solution and performing electrospinning experiments with the low EW PFSA polymers.

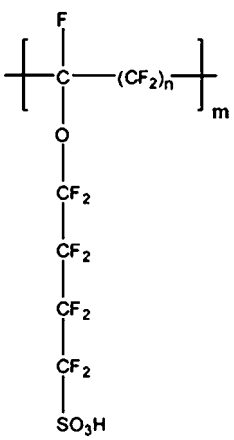

Fig. 1 The chemical structure of 3M Corporation perfluorosulfonic acid ionomer employed in the present work (for 825 EW polymer, n = 10; for 733 EW polymer, n = 8).

A 20.4 wt% solution of 825 EW PFSA in 1-propanol/water (2/1 wt/wt) and a 42.5 wt% solution of 733 EW PFSA in methanol/water (4/1 wt/wt) were provided by 3M Corporation (St. Paul, MN). Poly(ethylene oxide) (PEO) (MW 300,000 g/mol; CAS number 25322-68-3) was purchased from Alfa Aesar (Ward Hill, MA) and PEO with a molecular weight of 1,000,000 g/mol was purchased from Sigma-Aldrich. The PEOs were dissolved in the same mixed solvents (1-propanol/water or methanol/water) as the PFSA solutions at a concentration of 10 wt%. The proper amounts of the PFSA and PEO solutions were mixed together to prepare three sets of electrospinning solutions. In one set of solutions, the weight ratio of 825 EW PFSA to PEO (300 kDa MW) ranged from 50/50 to 99/1, where the total polymer concentration in solution was between 5 wt% and 15 wt%. A second set of electrospinning solutions was prepared from 825 EW PFSA and 1,000 KDa MW PEO, where the total polymer concentration was 15 wt%, for PFSA/PEO weight ratios of between 99.8/0.2 and 99.5/0.5. A third set of electrospinning solutions was prepared from 733 EW PFSA and 1,000 KDa MW PEO, where the total polymer concentration in solution was between 5 wt% and 30 wt%, for a single PFSA/PEO weight ratio of 99/1.

Electrospinning of PFSA (825 and 733 EW) with PEO

PFSA (825 EW)/PEO (300 KDa MW) solutions with 5–15 wt% total polymer concentration and PFSA/PEO weight ratios of between 50/50 and 99/1 were electrospun at the following conditions: 4.0–12.0 kV applied voltage between the collector and the spinneret, 8 cm spinneret-to-collector distance, and 0.15 mL/h solution flow rate. PFSA (825 EW)/PEO (1,000 KDa MW) solutions with 15 wt% total polymer concentration and PFSA/PEO weight ratios of between 99.8/0.2 and 99.5/0.5 were electrospun at the following conditions: 12.0 kV applied voltage between the collector and the spinneret, 8 cm spinneret-to-collector distance, and 0.15 mL/h solution flow rate. PFSA (733 EW)/PEO (1,000 KDa MW) (99/1 wt/wt) solutions with

5–30 wt% total polymer were electrospun at the following conditions: 8.0–12.0 kV applied voltage between the collector and the spinneret, 6 cm spinneret-to-collector distance, 0.30 mL/h solution flow rate. The drum fiber collector rotated at 1,000 rpm and moved laterally at 25 cm/s for all PFSA electrospinning experiments.

Annealing nanofiber mats with simultaneous fiber welding

825 EW PFSA mats were annealed at 140 °C for 5 min and 733 EW PFSA mats were annealed at 180 °C for 5 min (these annealing conditions were provided by 3M Corporation[17]). All fiber mats were annealed under vacuum. During the annealing step, intersecting fibers were welded to one another, as will be discussed below in the Results and Discussion section.

Compacting the mats

The annealed and welded mats were mechanically compacted between two Kapton® films at room temperature, using a standard bench-top hydraulic press (3912, Carver Inc.). The applied pressure was in the range of 2,000 psi to 10,000 psi and the time was 5 s for each compaction (a higher pressure produced more compaction and a higher fiber volume fraction, as will be discussed below).

Mat impregnation with inert polymer

The interfiber voids in annealed, welded, and compacted PFSA mats were filled completely with an inert, hydrophobic, and UV-crosslinkable liquid pre-polymer, Norland Optical Adhesive (NOA) 63. To impregnate, a mat was immersed in NOA 63 and air trapped in pores of the mat was removed by applying a vacuum for 1 h (at 45 °C). The mat was then removed from the vacuum oven and the surfaces of the mat were wiped clean of excess NOA. The NOA was then crosslinked by exposing the impregnated mats to UV light (365 nm); 1 h for each side, under a N_2 environment.

SEM study

The physical characteristics of nanofiber mats (fiber morphology and fiber diameter distribution) were determined using high resolution scanning electron microscopy (Hitachi Field Emission Scanning Electron Microscope S-4500). To image a mat cross-section, dry membranes were manually fractured after cooling in liquid nitrogen for 1 min. All specimens were sputter-coated with palladium (5 nm thickness). The fiber diameter distribution in a mat was analyzed by ImageJ, an image processing software, made available by the National Institute of Health (NIH; http://rsbweb.nih.gov/ij/index.html). At least 50 fibers were randomly selected from each of the micrographs for diameter measurements. A number-average fiber diameter distribution was then computed.

Fiber volume fraction and mat density

The fiber volume fraction (mat density) was calculated as the measured density of a given mat divided by the density of a homogeneous film prepared from the same polymer by solution casting (with full annealing),

$$\text{fiber volume fraction} = \frac{\text{density of fiber mat}}{\text{density of homogeneous film}} \quad (1)$$

Acid-water post-treatment

Prior to all measurements, PFSA nanofiber network composite membranes were boiled in 1M H_2SO_4 and water for 1 h each to remove traces of PEO. The membranes were then stored in water at room temperature until further use.

Proton conductivity

Membrane samples were dried in air for 16 h and then equilibrated in liquid water or a given water vapor atmosphere. The proton conductivity of water vapor equilibrated membrane samples was measured in the lateral (in-plane) direction by an AC impedance technique using a BekkTech, four-electrode cell (BT110, BekkTech LLC). An environmental chamber (SH-241, Espec Corp.) was employed to control humidity and temperature of the sample. The testing temperature was 80 °C and the relative humidity ranged from 30% RH to 80% RH. Proton conductivity was calculated from the following relationship:

$$\text{conductivity} = \frac{\text{s}}{\text{R} \times \text{w} \times \delta} \quad (2)$$

where, s is the spacing between the two electrodes (0.425 cm), $R[\Omega]$ is the measured resistance between the two electrodes, w is the width of the membrane sample (typically 0.40 cm), and δ[cm] is the wet membrane thickness (nanofiber composite membranes were typically 90–120 μm in wet thickness).

Water uptake from liquid

Equilibrium liquid water swelling of membranes was determined at room temperature, as the weight percent of absorbed water in the membrane (using the dry membrane as a reference). Membranes were kept in water for at least 72 h prior to a measurement to insure full equilibrium. After equilibration, membranes were weighed, then dried completely at 60 °C for 2 h and then at 90 °C for 16 h, and re-weighed. Membrane water swelling was determined according to the following equation:

$$\text{water sweling (\%)} = \frac{\text{m}_{\text{wet}} - \text{m}_{\text{dry}}}{\text{m}_{\text{dry}}} \times 100 \quad (3)$$

where, m_{wet} and m_{dry} are the weights of a water swollen and dry membrane sample, respectively.

Mechanical tests

Tensile stress-strain tests were performed using a Dynamic Mechanical Analyzer (DMA 2980, TA Instruments). Rectangular strips (40 × 3 mm^2) were cut from membrane samples and tested at room temperature. Prior to testing, the samples were equilibrated in liquid water for 24 h. Based on the stress-strain curves, the following mechanical properties were determined: strain at break, Young's modulus, and proportional limit stress.[18]

Differential scanning calorimetry (DSC)

Thermal characteristics of PFSA/PEO blends were determined using differential scanning calorimeter (DSC, TA Instruments Q100) equipped with a refrigerated cooling accessory. Nitrogen was used as a purge gas. Samples were enclosed in aluminium pans and heated from 70 °C to 200 °C at a rate of 10 °C/min.

Results and discussion

Electrostatic interactions in polyelectrolyte solutions limit the number of entanglements between polymer chains, and in this way, reduce electrospinnability of charged polymers. One approach to increase the entanglement of polymer chains is to increase the solution concentration but that frequently leads to an overly high viscosity which also makes electrospinning impossible. Another way to make a weakly entangled polymer solution electrospinnable is through addition of a high molecular weight polymer which then serves as a carrier. Thus, it has been shown in the literature that a carrier polymer such as poly(vinyl alcohol), poly(ethylene oxide) or poly(acrylic acid) can be used to electrospin perfluorosulfonic acid polymers (*e.g.*, Nafion) into nanofibers. For the case of polyethylene oxide (PEO), a carrier concentration of at least 16 wt% was required to electrospin Nafion nanofiber. In the present study, we sought to better understand PEO-PFSA interactions during electrospinning and to decrease the required amount of PEO for perfluorosulfonic acid polymer electrospinning.

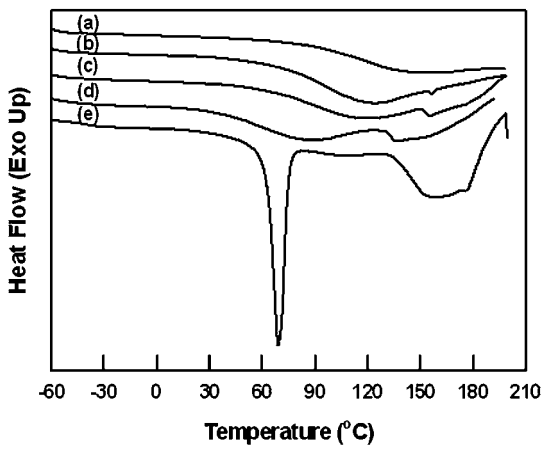

Fig. 2 DSC thermograms for PFSA/PEO blends of varying PEO content. (a) 0% PEO; (b) 1 wt% PEO; (c) 5 wt% PEO; (d) 10 wt% PEO; (e) 50 wt% PEO. Data are the first heating curves under N_2 at a heating rate of 10 °C/min.

As shown by the DSC scans of homogeneous (dense) solution-cast films composed of PFSA/PEO blends in Fig. 2, PEO is completely miscible with 825 EW PFSA up to 10 wt%, as revealed by the lack of a melting peak in the thermogram. At 50 wt% PEO, some immiscibility is evidenced by the presence of a strong endotherm around 60 °C. The observed favorable interactions originate from hydrogen bonding between the sulfonic acid groups of PFSA and the lone-pair electrons of the ether oxygens in PEO.[19]

To further study PEO-PFSA interactions and to develop a post-electrospinning PEO removal procedure, a series of proton conductivity experiments were made on dense solution cast PFSA/PEO films, all of which were annealed for 5 min at 140 °C (the normal annealing conditions for a solution cast 825 EW PFSA membrane). PEO is water soluble, so its removal from an electrospun mat or dense PFSA membrane was not expected to present any serious difficulty. Additionally, PEO may undergo degradation during membrane annealing due to the highly acidic PFSA environment, leading to a molecular weight decrease and the eventual formation of volatile dioxane. In the present study, PEO was removed from a PFSA membrane by boiling the sample in 1.0 M sulfuric acid for one hour followed by boiling in water for one hour (this is the normal pretreatment sequence for a neat Nafion membrane). To test this procedure, in-plane membrane conductivity measurements were made before and after PEO removal. As can be seen by the results in Table 1, there was a substantial loss in conductivity due to the presence of PEO in the recast PFSA/PEO dense films; prior to PEO removal, the in-plane conductivity at 80 °C and 50% RH was 0.041 and 0.036 S/cm for films containing 0.3 wt% PEO (1,000 KDa MW) and 1 wt% PEO (300 KDa MW), respectively *vs.* 0.055 S/cm for a neat recast membrane with no PEO. The loss in conductivity upon PEO addition was attributed to proton immobilization by the basic either oxygen sites of PEO. After boiling in acid and then water, the conductivity was fully recovered (0.056 and 0.054 S/cm for the two films listed in Table 1).

PFSA/PEO nanofiber electrospinning

733 EW and 825 EW PFSA polymers were electrospun separately into nanofiber mats. Changes in nanofiber morphology with PEO content and molecular weight and with the total polymer concentration of the electrospinning solution were studied. The materials used in these experiments were as

Table 1 Removal of the PEO component from recast PFSA/PEO dense films, as evidenced by the recovery of proton conductivity after boiling in acid and water

	Proton conductivity at 80 °C and 50% RH (S/cm)	
	PFSA/PEO (99.7/0.3 wt ratio; 1,000 KDa MW PEO)	PFSA/PEO (99/1 wt ratio; 300 KDa MW PEO)
Cast and Annealed film	0.041	0.036
Film that was Boiled in 1.0 M H_2SO_4 and water (one hour each)	0.056	0.054
Cast and annealed film without the addition of PEO	0.055	

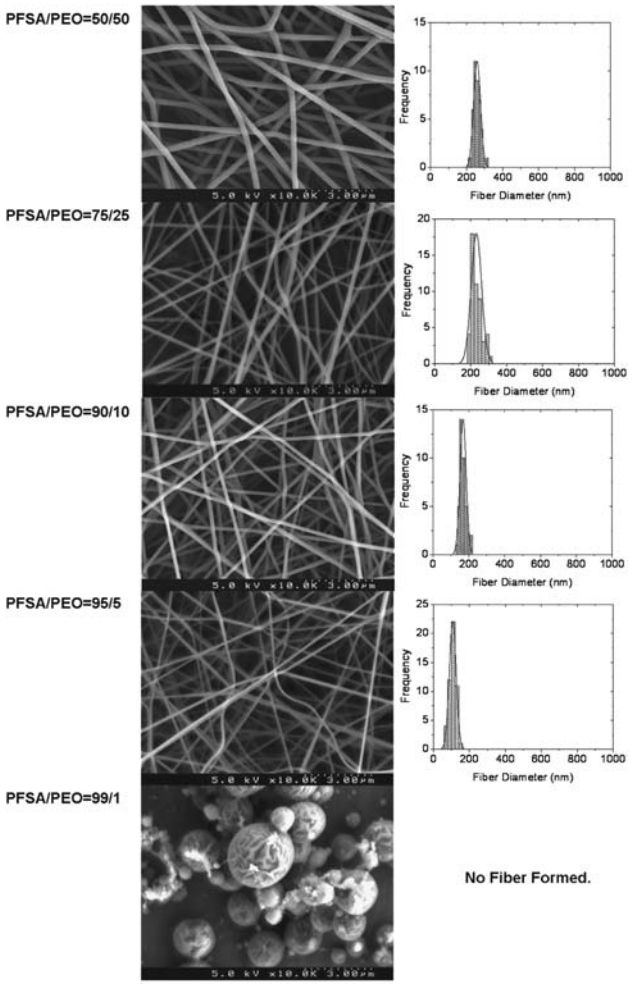

Fig. 3 SEM images of electrospun mats from 5 wt% solutions of different PFSA/PEO weight ratio (where the solvent was a 2/1 wt ratio of 1-propanol/water). Fiber diameter distributions are shown in the histograms on the right.

follows: 3M PFSA (825 EW), PEO (300 KDa MW), and a 1-propanol/water mixed solvent (2 : 1 by wt.). Fiber mats were prepared using electrospinning solutions with different PFSA/PEO weight ratios (50/50, 75/25. 90/10, 95/5 and 99/1), where the total polymer concentration (PFSA + PEO) was either 5 wt% or 10 wt%. It was observed that a higher electric potential was required for fiber generation as the concentration of PEO in the electrospinning solution decreased from 50% (4 kV potential required) to 1% (8 kV potential), where the spinneret-to-collector distance (8 cm) and solution flow rate (15 mL/h) were held constant. SEM images of fiber mats and histograms of the fiber diameter distribution are shown in Fig. 3 for electrospinning solutions with different PFSA/PEO weight ratios, where the total polymer concentration was 5 wt%. All of the mats were of good quality with no beading, except the 99/1 spinning solution. SEM images of mats electrospun from 10 wt% solutions are shown in Fig. 4, where again, the average fiber diameter decreased with decreasing PEO content (no data is shown for 50/50 PFSA/PEO because the solution was too viscous to electrospin). Also, with a 10 wt% polymer solution, it was possible to create good-quality fibers with no beads from a 99/1 PFSA/PEO solution. The more

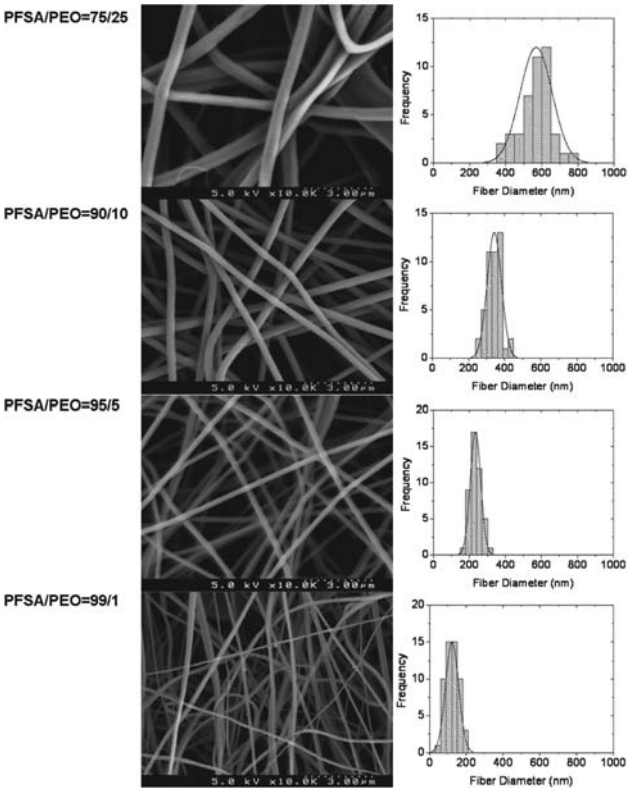

Fig. 4 SEM images of electrospun mats from 10 wt% solutions with different PFSA/PEO weight ratios (2/1 wt ratio of 1-propanol/water). Fiber diameter distributions are shown in the histograms on the right.

dilute spinning solution produced fibers of lower diameter at a given PFSA/PEO ratio. Thus, the smallest fiber diameter (107 nm) for the 825 EW PFSA polymer was obtained with a 5 wt% total polymer spinning solution, where the PFSA/PEO wt ratio was 95/5.

The minimum amount of 300 KDa MW PEO necessary to electrospin PFSA polymer was 1% (see Fig. 4), which is considerably less than what is reported in the literature.[15,16] In an attempt to determine if the required amount of PEO carrier polymer for PFSA electrospinning could be further reduced, a PFSA/PEO solution with 1,000 KDa MW PEO was electrospun at PEO concentrations of 0.2, 0.3, and 0.5 wt%. The electrospinning conditions were as follows: 12 kV of electric potential, 8 cm of spinneret-to-collector distance, and 0.15 mL/h of solution flow rate. SEMs of the resulting membranes are shown in Fig. 5. A bead-on-fiber morphology was observed for 0.2 wt% PEO, whereas well-formed nanofibers (with an average diameter of approximately 150 nm) were obtained at the two higher PEO concentrations. The high MW PEO produced a higher solution viscosity, so less PEO was required for PFSA electrospinning.

The total polymer content (PFSA + PEO) of the electrospinning solution was found to be equally critical as the carrier polymer content itself, when attempting to electrospin PFSA mats with well-formed nanofibers. At a low concentration, the solution viscosity was too low and the number of entanglements was insufficient for a stable fiber to form. When the concentration was too high, the applied electrostatic field could not overcome surface tension and a fiber could not be ejected from the

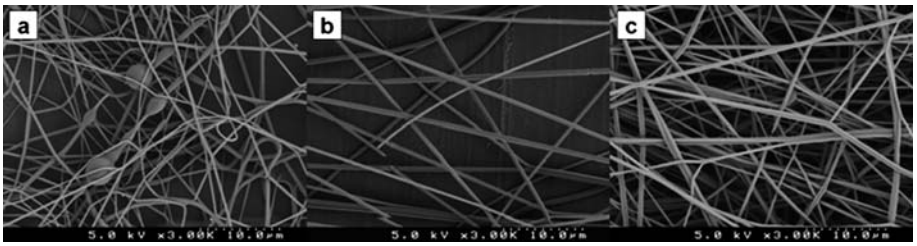

Fig. 5 SEM images of nanofiber mats made by cospinning 825 EW PFSA with PEO. The PFSA/PEO wt ratios in the spinning solutions are (a) 99.8/0.2, (b) 99.7/0.3, and (c) 99.5/0.5.

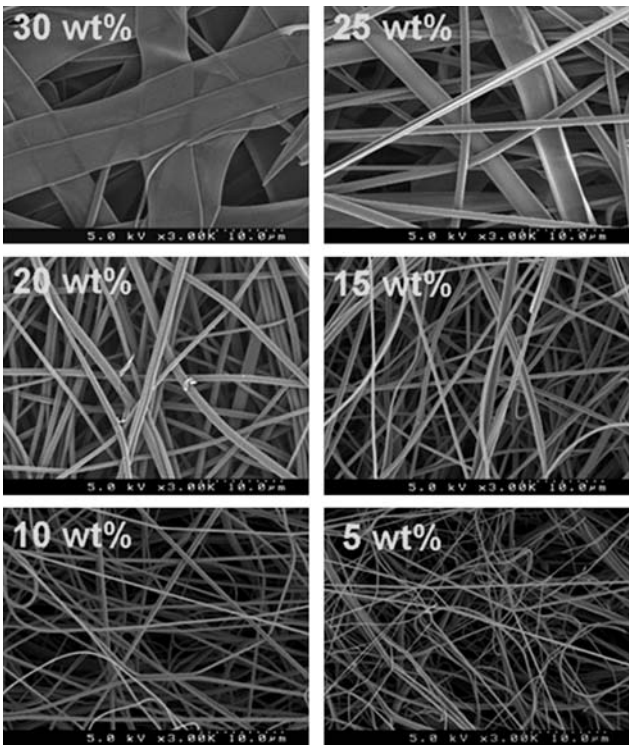

Fig. 6 SEM images of 733 EW PFSA nanofiber mats electrospun using 1 wt% PEO as the carrier, where the total polymer concentration in solution (PFSA + PEO) is varied from 5 wt% to 30 wt%.

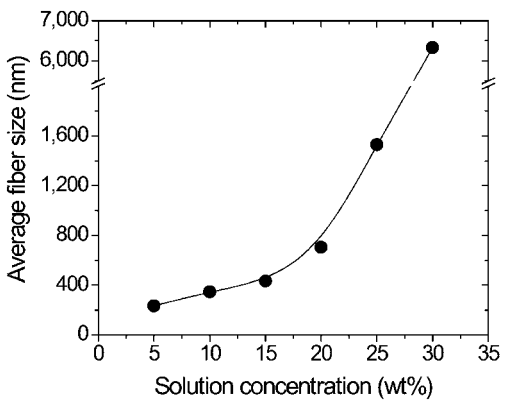

Fig. 7 Dependence of fiber diameter on the electrospinning solution concentration (PFSA + PEO) for 733 EW PFSA polymer, where the PEO carrier concentration was 1 wt%.

spinneret needle. Total polymer concentration effects were investigated using 733 EW PFSA polymer with 1 wt% PEO (1,000 KDa MW). As can be seen from the SEMs in Fig. 6, the fiber morphology transitioned from cylindrical fibers to flattened ribbons as the total polymer concentration increased (data is shown for the case where the 1,000 KDa MW PEO concentration in the spinning solution was held constant at 1 wt%). The dependence of average fiber diameter/width (as determined from the SEMs) on total polymer concentration is plotted in Fig. 7. Thus, at 30 wt% total polymer (with 1% PEO carrier), wide and flat ribbons were spun, with a width of about 6.4 μm (6,400 nm). With 25 wt% polymer, ribbons and fibers were made, where the ribbons were 1.5 μm wide. At a polymer concentration ≤ 20 wt%, only fibers were produced, with an average diameter of 703 nm (20 wt%), 433 nm (15 wt%), 390 nm (10 wt%), and 200 nm (5 wt%).

Processing nanofiber mats into membranes

In order to convert a PFSA/PEO nanofiber mat into a defect free ion-exchange (fuel cell) membrane, the following processing steps were performed: (i) annealing the PFSA polymer at 140 °C (for 825 EW PFSA) or 180 °C (for mats with 733 EW PFSA nanofibers), (ii) mechanically compacting the mats to increase the volume fraction of nanofibers (as-spun mats typically had a fiber volume fraction of 0.20–0.25 which was too low for high proton transport rates), (iii) imbibing an inert polymer, Norland Optical Adhesive (NOA) 63, into the mats to fill entirely the void volume between nanofibers, followed by UV crosslinking of the NOA (at 365 nm wavelength and room temperature for 120 min; 60 min for each side of the membrane), and (iv) removing PEO by boiling the membrane in 1.0 M H_2SO_4 for one hour and deionized water for one hour.

For PFSA nanofiber mats, intersecting fibers could be welded to one another during the polymer annealing step. The effect of annealing time on interfiber welding and mat structure is shown in Fig. 8 (for a mat composed on 825 EW PFSA with 1 wt% PEO). The results show that at least 2 min were required for a significant number of inter-fiber welds to form at 140 °C (2 min was also a sufficient time for 825 EW polymer annealing). After annealing/welding, there was a small increase in fiber diameter (~10%) and an increase in the volume fraction of fibers (from 0.22 to 0.45). For nanofiber mats containing more than 25 wt% PEO, the fiber morphology degraded during annealing/welding. Fig. 9 shows the SEMs from such a mat before and after annealing at 140 °C for 5 min, where nearly complete fusion of the entire nanostructure occurred with closure of most interfiber voids. The creation of welds at low PEO contents and the

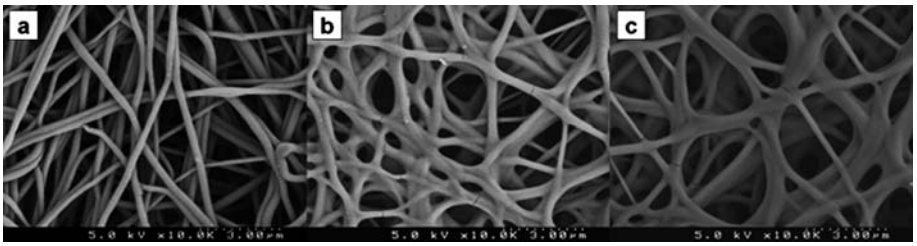

Fig. 8 SEM images of an 825 EW PFSA fiber mat annealed at 140 °C for (a) 1, (b) 2, and (c) 5 min.

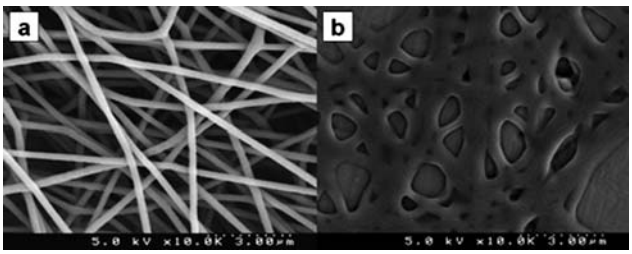

Fig. 9 SEM images of 825 EW PFSA + PEO (50wt% PEO) nanofiber mat (a) before and (b) after annealing (annealing conditions: 140 °C for 5 min).

unacceptable transformation of the mat morphology at high PEO concentrations were attributed to the low melting point (65 °C) of PEO.

The initial mat density of the electrospun mats was relatively low, on the order of 20–25%. It increased during the welding/annealing step to 35–45%, but this was still well below the desired level of 60–85% required for highly conductive membranes. To increase the mat density to a required value, mechanical compression in a hydraulic press was employed. The process was carried out at room temperature for 5 s under constant pressure. Since the 733 EW and 825 EW PFSA polymers are highly hygroscopic and absorbed water from lab air, the annealed mats were dried at 100 °C under vacuum for 24 h prior to densification. The effect of compaction pressure on fiber volume fraction in the 733 EW and 825 EW PFSA mats is shown in Fig. 10. The two trend lines run nearly parallel and the mat density appears to level-off at pressures > 8000 Psi. After compaction at 8,000 psi,

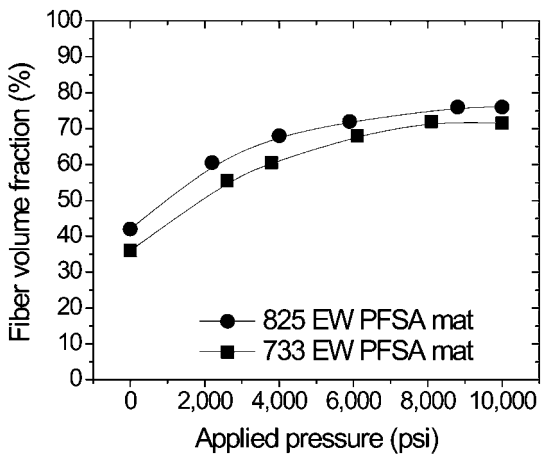

Fig. 10 The effect of compaction pressure on mat density. Densification of dry mats was carried out at room temperature in a hydraulic press.

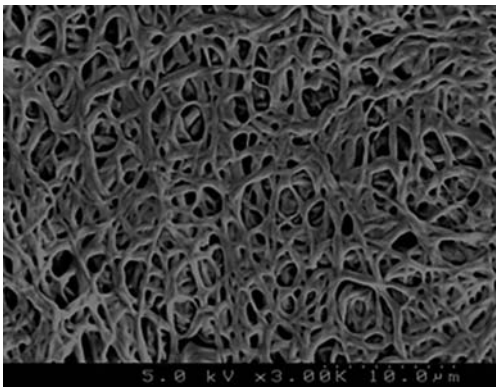

Fig. 11 SEM images of an annealed, welded, and densified mat composed of 825 EW PFSA nanofibers with 1 wt% PEO (300 KDa MW) as the carrier prior to impregnation with NOA 63.

the initial fiber volume fraction roughly doubles to 74% (733 EW) and 77% (for 825 EW). A SEM micrograph of an annealed, welded, and densified nanofiber mat electrospun from EW 825 PFSA with 1% PEO is shown in Fig. 11.

PFSA-NOA composite membrane properties

Proton conductivity and water uptake

The in-plane proton conductivity of water-vapor equilibrated membranes was measured at 80 °C for a relative humidity between 30% and 80%. The results are shown in Fig. 12 for a 733 EW nanofiber membrane with a fiber volume fraction of 0.70, an 825 EW nanofiber membrane with a fiber volume fraction of 0.74, and for Nafion 212 as a reference. As expected, given its higher sulfonic acid group concentration, the conductivity of the PFSA EW 733 nanofiber composite membrane was greater than that of the EW 825 membrane at all humidity levels tested. Through-plane proton conductivity measurements were not carried out (but in a prior study with sulfonated polysulfone nanofiber composite membranes,[10] through-plane and in-plane conductivities were found to be the same). Both nanofiber membranes were more conductive than Nafion 212. Also, the proton conductivity of the nanofiber composite membranes increased linearly with PFSA nanofiber volume fraction, whereas gravimetric water swelling was less than expected, based on the volume fraction of ionomer. An example of this conductivity and water swelling behavior is shown in Fig. 13, for a nanofiber composite membrane with 733 EW PFSA polymer. The observed linear dependence of conductivity on PFSA volume fraction (which should extend over the entire range of PFSA volume

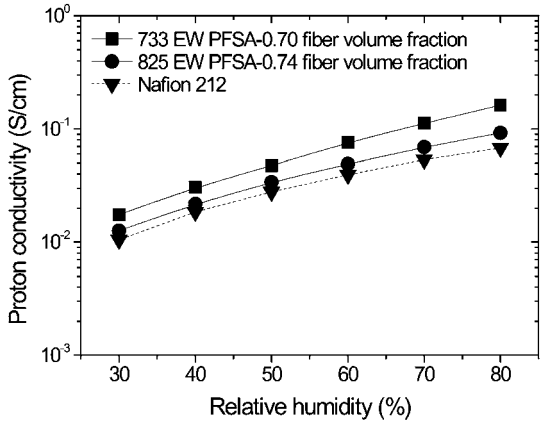

Fig. 12 Variation of in-plane proton conductivity with relative humidity at 80 °C for two nanofiber composite membranes and for Nafion 212. Thickness of the dried membranes is 75 μm, 82 μm and 53 μm for 733 EW PFSA and 825 EW nanofiber composite membranes and for Nafion 212, respectively.

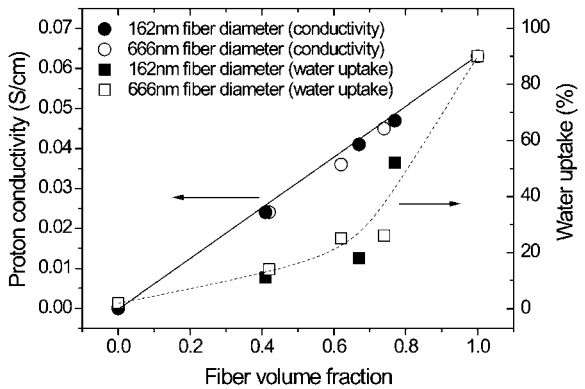

Fig. 13 In-plane proton conductivity and water uptake of nanofiber composite membranes (733 EW PFSA nanofibers), where the average fiber diameter was 162 nm or 666 nm (proton conductivity was measured at 80 °C and 50% RH; water uptake was measured at 25 °C in liquid water).

fractions) is highly beneficial and is due to the presence of a continuous network of proton-conducting nanofibrous paths which span the membrane thickness. The absence of percolation effects in nanofiber membranes has already been demonstrated and discussed in an earlier paper.[10] Water swelling and proton conductivity of nanofiber composite membranes (with a fiber volume fraction in the 0.6–0.7 range) compare well with published data on Gore-Select® PFSA composite membranes[20] (18% water swelling and 0.041 S/cm conductivity for a nanofiber composite membrane with a fiber volume fraction of 0.67 *vs.* 32% gravimetric water swelling and 0.053 S/cm conductivity for Gore-Select).

Mechanical properties

One of the main advantages of the composite nanofiber membranes is the expected improvement in mechanical strength combined with high proton conductivity. In classical blends or composites, an improvement in tensile or compressive properties is observed when a substantial amount of the reinforcing component is introduced into the membrane (usually 40–60 vol% of the reinforcement polymer is required). Due to the nano-level architecture of the nanofiber composite membranes, there is significantly better dispersion of the reinforcement polymer throughout the membrane, with considerably greater interfacial area between the PFSA and NOA, which should lead to a stronger composite material, as compared to macro-composites or blends.

Stress-strain curves for membrane samples equilibrated in room temperature liquid water for 24 h and then subjected to Dynamic Mechanical Analysis (DMA) testing are shown in Fig. 14. Values of Young's modulus and the proportional limit stress (PLS) are listed in Table 2 (also listed in the table, for comparison purposes, are the Young's modulus and PLS of Nafion[12]). The resulting order for Young's modulus was as follows: UV cured NOA63 homogeneous film > 825 EW PFSA nanofiber network membrane > Nafion> 733 EW PFSA nanofiber network membrane > 825 EW PFSA homogeneous film > 733 EW PFSA homogeneous film. The strengthening effect of the NOA63 in the nanofiber composite membranes is clearly seen. Nanofiber composite membranes exhibited a higher value of the Young's modulus than that of dense, recast films. Elongation at break was lower for the composite membranes, as compared to the dense films, with the 825 EW-based membranes showing the

Table 2 Young's modulus and proportional limit stress (PLS) of 3M PFSA films, 3M PFSA nanofiber network membranes, and a UV cured NOA63 film at 25 °C (all equilibrated in water)

Sample	Young's modulus (MPa)	PLS (MPa)
3M PFSA (733 EW) film	45.4	3.9
3M PFSA (825 EW) film	77.6	6.2
3M PFSA (733 EW)/NOA63	161.6	7.7
3M PFSA (825 EW)/NOA63	270.5	10.1
UV cured NOA63 film	835.0	24.7
Nafion[12]	190.0	10.0

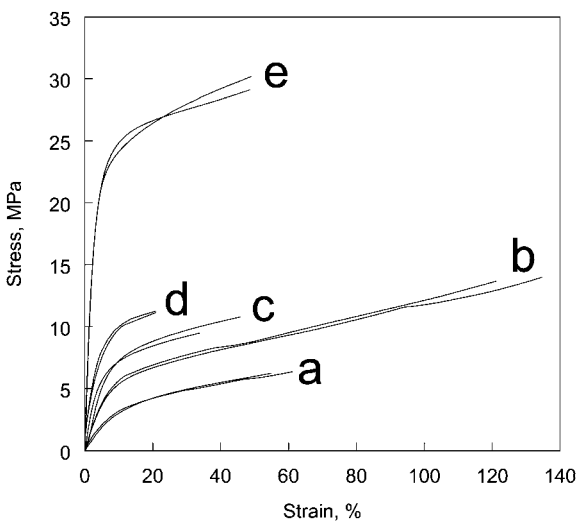

Fig. 14 Stress-strain curves of membrane samples at 25 °C, in the wet state: (a) 733 EW PFSA homogeneous film, (b) 825 EW PFSA homogeneous film, (c) 733 EW PFSA nanofiber network membrane (0.70 fiber volume fraction), (d) 825 EW PFSA nanofiber network membrane (0.73 fiber volume fraction) and (e) UV-crosslinked NOA 63.

most pronounced difference. From the results in Fig. 14 and the data listed in Table 2, it can be concluded that the embedded nanofiber membranes exhibited superior mechanical properties, as compared to the homogeneous PFSA films, where the incorporation of 27–30% NOA nearly doubled the proportional limit stress, with a 3.5-fold increase in Young's modulus.

Conclusion

Two low equivalent weight perfluorosulfonic acid (PFSA) polymers (825 EW and 733 EW) from 3M Corporation were successfully electrospun into nanofibers by adding a small amount (typically 1 wt% and in some cases as little as 0.3 wt%) of high molecular weight poly(ethylene oxide) (PEO) as a carrier. The electrospun fiber morphology transitioned from cylindrical filaments to flat ribbons as the total concentration of PFSA + PEO carrier in solution increased from 5 wt% to 30 wt%. PFSA nanofiber mats were transformed into defect-free dense membranes (based on visual inspection of SEMs) using a four-step procedure comprising: (i) annealing the PFSA polymer at 140 °C (for 825 EW) or 180 °C (for 733 EW) during which time intersecting fibers were welded to one another at cross points to create a 3-dimensional interconnecting fiber network, (ii) mechanically compacting the mats for five seconds to increase the volume fraction of nanofibers to ~75%, (iii) imbibing an inert polymer, Norland Optical Adhesive (NOA) 63, into the mats to fill completely the void space between nanofibers, followed by UV crosslinking of the NOA (at 365 nm wavelength and room temperature for 120 min; 60 min for each side of the membrane), and (iv) removing the poly(ethylene oxide) carrier polymer by boiling the membrane in 1.0 M H_2SO_4 for one hour and in deionized water for one hour. The resulting membranes exhibited higher proton conductivities than those of a commercial Nafion 212 membrane at humidities ranging from 30% to 80%. Thus, at 80 °C and 80% relative humidity, the conductivity with 733 EW PFSA nanofibers was 0.16 S/cm (*vs.* 0.068 S/cm for Nafion 212) and at 80 °C and 50% relative humidity, the conductivity was 0.048 S/cm (*vs.* 0.028 S/cm for Nafion 212). The proton conductivity of 825 EW and 733 EW nanofiber composite membranes increased linearly with the PFSA nanofiber volume fraction, whereas gravimetric water swelling was less than expected, based on the volume fraction of ionomer. The low swelling of the nanofiber composite membranes should be beneficial for fuel cell applications. For example, at an 825 EW PFSA nanofiber volume fraction of 0.67, the swelling in liquid water was only 18%, whereas the membrane conductivity was high (*e.g.*, 0.041 S/cm at 80 °C and 50% relative humidity). There was also a significant improvement in the mechanical properties of the nanofiber composite membranes, as compared to recast homogeneous PFSA films, with a 3.5-fold increase in Young's modulus and about a 2-fold increase in the proportional limit stress.

Acknowledgements

The authors gratefully acknowledge the financial support of the U.S. Department of Energy, Energy Efficiency and Renewable Energy Program (Grant No. DE-FG36-06GO16030). The authors also thank Dr. Steven Hamrock at 3M Corporation for providing the PFSA polymers used in this study.

References

1 M. Litt and J. Kang, *presented in part at the 213th Electrochemical Society Meeting*, Phoenix, AZ, May, 2008.
2 R. Nolte, K. Ledjeff, M. Bauer and R. Mülhaupt, *J. Membr. Sci.*, 1993, **83**, 211–220.
3 H. Wang, A. S. Badami, A. Roy and J. E. McGrath, *J. Polym. Sci., Part A: Polym. Chem.*, 2007, **45**, 284–294.
4 H. Ghassemi, J. E. McGrath and T. A. Zawodzinski, *Polymer*, 2006, **47**, 4132–4139.
5 S. Swier, V. Ramani, J. M. Fenton, H. R. Kunz, M. T. Shaw and R. A. Weiss, *J. Membr. Sci.*, 2005, **256**, 122–133.
6 V. Baglio, A. S. Aricò, V. Antonucci, I. Nicotera, C. Oliviero, L. Coppola and P. L. Antonucci, *J. Power Sources*, 2006, **163**, 52–55.
7 K. M. Nouel and P. S. Fedkiw, *Electrochim. Acta*, 1998, **43**, 2381–2387.
8 F. Liu, B. Yi, D. Xing, J. Yu and H. Zhang, *J. Membr. Sci.*, 2003, **212**, 213–223.
9 C. Mittelsteadt, *Hydrogen, Fuel Cells and Infrastructure Technologies Annual Progress Report*, 2009.
10 J. Choi, K. M. Lee, R. Wycisk, P. N. Pintauro and P. T. Mather, *Macromolecules*, 2008, **41**, 4569–4572.
11 J. Choi, K. M. Lee, R. Wycisk, P. N. Pintauro and P. T. Mather, *J. Electrochem. Soc.*, 2010, **157**, B914–B919.
12 K. M. Lee, J. Choi, R. Wycisk, P. N. Pintauro and P. T. Mather, *ECS Trans.*, 2009, **25**, 1451–1458.
13 S. J. Hamrock and M. A. Yandrasits, *J. Macromo. Sci, Part C: Polym. Rev.*, 2006, **46**, 219–244.
14 M. Emery, M. Frey, M. Guerra, G. Haugen, K. Hintzer, K. H. Lochhas, P. Pham, D. Pierpont, M. Schaberg, A. Thaler, M. Yandrasits and S. Hamrock, *ECS Trans.*, 2007, **11**, 3–14.
15 A. Laforgue, L. Robitaille, A. Mokrini and A. Ajji, *Macromol. Mater. Eng.*, 2007, **292**, 1229–1236.
16 H. Chen, J. D. Snyder and Y. A. Elabd, *Macromolecules*, 2008, **41**, 128–135.
17 Private communication from S. Hamrock at 3M Corporation.
18 Y. Tang, A. Kusogulu, A. M. Karlsson, M. H. Santare, S. Cleghorn and W. B. Johnson, *J. Power Sources*, 2008, **175**, 817–825.
19 H.-L. Chen, C.-C. Ko and T.-L. Lin, *Langmuir*, 2002, **18**, 5619–5623.
20 J. Kolde, B. Baharm, M. S. Wilson, T. A. Zawodzinski and S. Gottesfeld, *Electrochemical Society Proceedings*, 1995, **95–23**, 193–201.

